

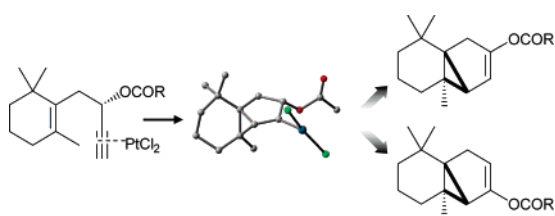
On Accounting for the Stereoselective Control of the Metal-Catalyzed Rautenstrauch Cyclopropanation by Computational Methods[§]

Elena Soriano^{*,†} and José Marco-Contelles[‡]

Laboratorio de Resonancia Magnética, Instituto de Investigaciones Biomédicas (CSIC), C/ Arturo Duperier 4, 28029-Madrid, Spain, and Laboratorio de Radicales Libres, IQOG (CSIC), C/ Juan de la Cierva 3, 28006-Madrid, Spain

esoriano@iib.uam.es

Received December 18, 2006



The mechanism of the intramolecular Pt(II)-catalyzed Rautenstrauch cyclopropanation and the stereochemical implications have been investigated by computational methods. The reaction takes place through a cyclopropanation step preceding the cleavage of the C–O bond, thus ensuring the transfer of chiral information from the stereogenic propargylic center. Our results agree with experimental findings and account for the origin of the substrate-dependent selectivity on the basis of subtle electronic effects and steric interactions in the cyclopropanation transition-state structure.

In the past few years, the transition-metal-catalyzed Rautenstrauch cycloisomerization has emerged as a powerful and efficient approach to transform propargylic esters into cyclic enones,^{1,2} important building blocks for the synthesis of natural products. This reaction is efficiently promoted by soft noble metal complexes, such as PtCl₂, Cu(I)-salts, Au(I)-salts, or AuCl₃. The complexation of the alkyne moiety to the metal complex triggers the attack by nucleophiles such as alkenes or carbonyl groups. This process has been described for the cycloisomerization of 1,3-³ and 1,4-enynes,⁴ but it is most

commonly applied for the cyclopropanation of 1,5- and 1,6-enynes to afford bicyclo[n.1.0]hex(or hept)-2-en-2-yl carboxylates.⁵

To date, three different reaction pathways have been postulated for the Rautenstrauch cyclopropanation process (formation of **D**, Scheme 1). The initial 1,2-acyl migration to form a vinyl-carbene intermediate (**C**, Scheme 1, path I), which undergoes cyclopropanation, has become the most widely accepted mechanism^{2,5} but is no longer tenable in view of new experimental^{6,7} and theoretical evidence (see below). Alternatively, a path following the inverse sequence of steps, that is, through an initial cyclopropanation by nucleophilic attack of the alkene, followed by a stepwise 1,2-acyl migration (Scheme 1, path II) has been formulated by us⁸ and was later also proposed and supported by Fürstner and Hannen to account for new stereochemical data.⁶ For racemic or enantiomerically pure unsaturated propargylic carboxylates, if the cyclopropanation step proceeds before the 1,2-acyloxy group migration, the stereochemical outcome should be dependent on the absolute configuration of the stereocenter being destroyed. Fürstner and Hannen⁶ have reported the PtCl₂ promoted Rautenstrauch cyclopropanation of conveniently functionalized, diastereo- and enantiomerically pure unsaturated propargylic acetates for the synthesis of (–)-cubebol (Scheme 2). In an independent work, Fehr and Galindo⁷ have used the same strategy for the same target and have described the PtCl₂, Ph₃PAuCl, or [Cu(CH₃CN)₄](BF₄) mediated Rautenstrauch cyclopropanation on identical, or related, pivaloates (Scheme 2). Very interestingly, in this case PtCl₂ gave the best chemical yields, with similar high diastereo- and enantioselectivity, thus, we have selected this catalyst to perform the study reported here. These are the first experimental findings^{6,7} which provide strong evidence for a remarkable transfer of chirality from the propargylic carbon to the newly formed stereocenters, pointing to a C–C bond formation event prior to the cleavage of the C–O bond, a fact that we had already advanced and proposed in a former work.⁸ While Fürstner and Hannen have invoked path II to justify these results, Fehr and Galindo have postulated a concerted C–C bond formation/C–O bond-breaking pathway (Scheme 1, path III).

In this manuscript, we have computationally analyzed the experimental findings by Fürstner and Hannen and by Fehr and Galindo^{6,7} in an effort to shed light on the mechanistic controversy described above. Theoretical calculations indicate that rotational barrier of the 1-acyloxy penta-1,3-diene chain

[§] Dedicated to Prof. Miguel Yus on the occasion of his 60th birthday.

[†] Instituto de Investigaciones Biomédicas.

[‡] IQOG.

(1) For pioneering work, see: Rautenstrauch, V. *J. Org. Chem.* **1984**, *49*, 950–952.

(2) (a) For a seminal paper, see: Mainetti, E.; Mouries, V.; Fensterbank, L.; Malacria, M.; Marco-Contelles, J. *Angew. Chem., Int. Ed.* **2002**, *41*, 2132–2135. (b) For a recent concept, see: Marco-Contelles, J.; Soriano, E. *Chem. Eur. J.* **2007**, *13*, 1350–1357.

(3) Zhang, L.; Wang, S. *J. Am. Chem. Soc.* **2006**, *128*, 1442–1443.

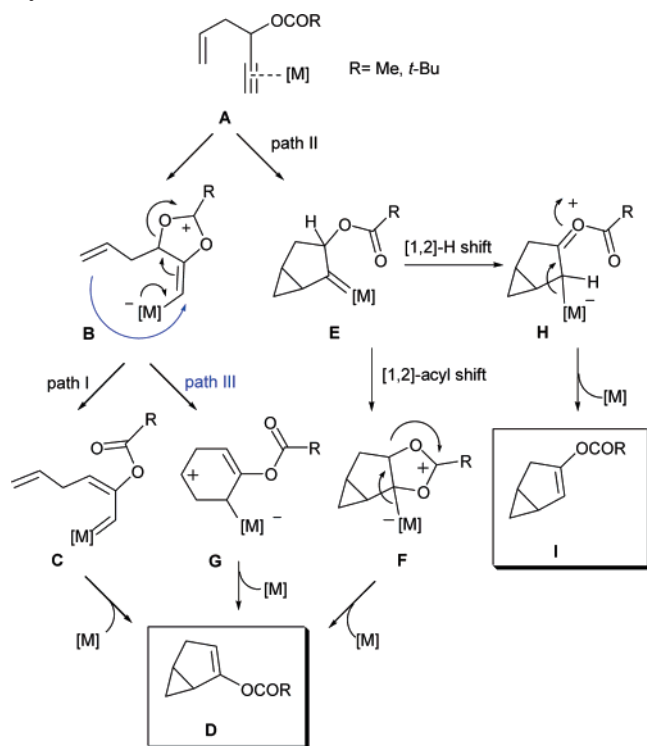
(4) (a) Marion, N.; Díez-González, S.; de Frémont, P.; Noble, A. R.; Nolan, S. P. *Angew. Chem., Int. Ed.* **2006**, *45*, 3647–3650. (b) Shi, X.; Gorin, D. J.; Toste, F. D. *J. Am. Chem. Soc.* **2005**, *127*, 5802–5803. (c) Prasad, B. A. B.; Yoshimoto, F. K.; Sarpong, R. *J. Am. Chem. Soc.* **2005**, *127*, 12468–12469.

(5) (a) Marco-Contelles, J.; Arroyo, N.; Anjum, S.; Mainetti, E.; Marion, N.; Cariou, K.; Lemièrre, G.; Mouries, V.; Fensterbank, L.; Malacria, M. *Eur. J. Org. Chem.* **2006**, 4618–4633. (b) Marion, N.; de Frémont, P.; Lemièrre, G.; Stevens, E. D.; Fensterbank, L.; Malacria, M.; Nolan, S. P. *Chem. Commun.* **2006**, 2048–2050. (c) Anjum, S.; Marco-Contelles, J. *Tetrahedron* **2005**, *61*, 4793–4803. (d) Gagosz, F. *Org. Lett.* **2005**, *7*, 4129–4132. (e) Fürstner, F.; Hannen, P. *Chem. Commun.* **2004**, 2546–2547. (f) Harrak, Y.; Blaszykowski, C.; Bernard, M.; Cariou, K.; Mainetti, E.; Mouries, V.; Dhimane, A. L.; Fensterbank, L.; Malacria, M. *J. Am. Chem. Soc.* **2004**, *126*, 8656–8657. (g) Mamane, V.; Gress, T.; Krause, H.; Fürstner, A. *J. Am. Chem. Soc.* **2004**, *126*, 8654–8655. (h) Fürstner, P.; Hannen, P. *Chem. Commun.* **2004**, 2546–2547. (i) Blaszykowski, C.; Harrak, Y.; Gonçalves, M. H.; Cloarec, J. M.; Dhimane, A. L.; Fensterbank, L.; Malacria, M. *Org. Lett.* **2004**, *6*, 3771–3774.

(6) Fürstner, A.; Hannen, P. *Chem. Eur. J.* **2006**, *12*, 3006–3019.

(7) Fehr, C.; Galindo, J. *Angew. Chem., Int. Ed.* **2006**, *45*, 2901–2904. (8) Soriano, E.; Ballesteros, P.; Marco-Contelles, J. *Organometallics* **2005**, *24*, 3182–3191.

SCHEME 1. Proposed Mechanisms for the Cycloisomerizations

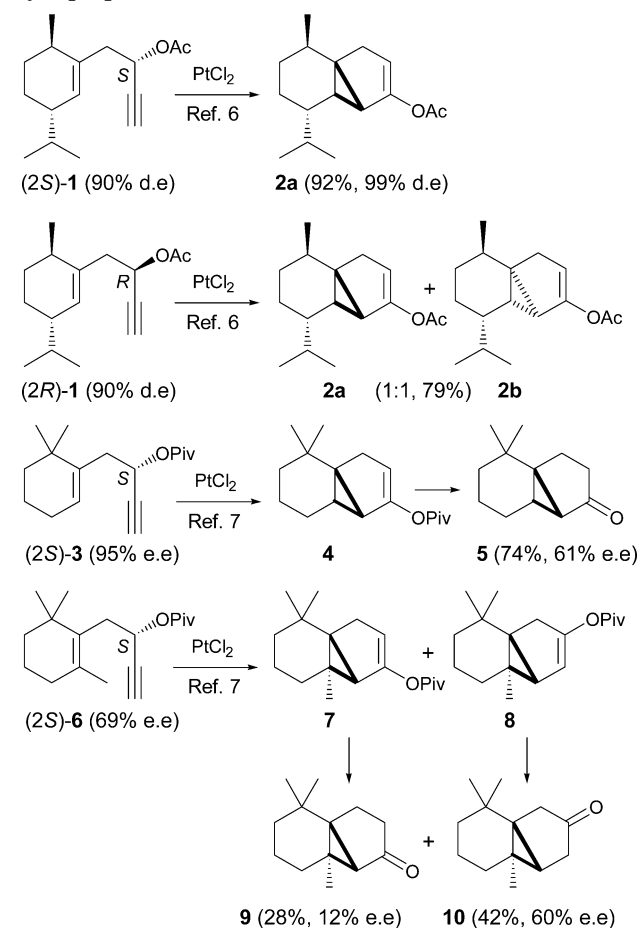


for the vinyl carbene intermediate **C** (Scheme 1) is favored relative to cyclization⁹ (see Figure S2, Supporting Information), so the chiral information would be lost, which excludes path I as operative route under these catalytic conditions.

To verify the hypothesis proposed by Fehr and Galindo (Scheme 1, path III), we have performed a detailed relaxed PES (potential energy surface) scan, selecting the involved C–C and C–O distances as independent coordinates, and varying them from 1.6 to 3.0 Å. The results clearly reveal that a transition structure involving the concerted C–O bond cleavage/C–C bond formation cannot be found, even supposing a high asynchronicity (see Figure S3, Supporting Information). Moreover, after a thorough search, we could not characterize the subsequent cyclized “half-rearranged” species **G** (Scheme 1, path III) as local minimum on the PES (in gas phase and in solution). This suggests that Fehr and Galindo’s proposal, closely related to Shi et al.’s,^{4b} can also be excluded as operative mechanism.

In this context, path II (Scheme 1) seems a plausible mechanistic picture that could justify the stereochemical outcome. The intrinsic π -stereofacial selectivity was analyzed by examining the key C–C bond formation step (**A** \rightarrow **E**). From the results shown in Table 1 for epimer (2*S*)-**1** (precursor **1**, *S* configuration at the propargylic position), it can be deduced that the cyclopropyl metal-carbenoid intermediate **E** resulting from cyclopropanation¹⁰ onto the β -face of the alkene (**a** series) is favored over the α -face attacking (**b** series) by 2 kcal mol⁻¹. In contrast, the (2*R*)-epimer undergoes cyclopropanation with similar activation barriers from the two faces (varying by

SCHEME 2. Enantioselective Rautenstrauch Cyclopropanation



0.5 kcal mol⁻¹) therefore suggesting no face selectivity. The cyclopropanation step for both substrates is highly exothermic indicating an irreversible character. These results agree with experimental evidence^{6,7} and suggest a kinetically determined stereoselectivity.

The origin of this kinetic preference was explored by inspecting the transition structures **TS** (Figure 1). The approach of the incoming alkyne group in (2*S*)-**1TS_b** is sterically impeded by the isopropyl moiety (H \cdots H distance of 2.112 Å, which is shorter than the sum of van der Waals radii, 2.4 Å). In contrast, a similar steric hindrance was not observed for the approaching to the opposite face, (2*S*)-**1TS_a**. Surprisingly, in this case the distance to the proton at the endocyclic CH moiety is longer (even by assuming a less favorable pseudoaxial conformation for the endocyclic CH proton, 2.652 Å). This effect, though significant, is insufficient to rationalize experimental observations, as **1** *R*-diastereoenriched furnished **2a** and **2b** as a 1:1 mixture of diastereomers.⁶

As can be seen in Figure 1, the ester group plays a key role in the case of the (2*S*)-isomer. A C–H \cdots O interaction between the ester oxygen and the alkene hydrogen atom (C–H \cdots O distance of 2.486 Å) was identified¹¹ in (2*S*)-**1TS_a** for the β -face attacking. Such an interaction was confirmed by the existence of a bond path between O and H atoms¹² (electron density at

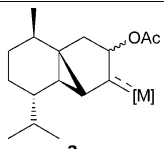
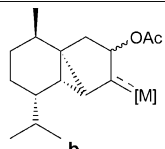
(9) Nieto-Faza, O.; Silva-López, C.; Álvarez, R.; de Lera, A. R. *J. Am. Chem. Soc.* **2006**, *128*, 2434–2437.

(10) For recent reviews, see: (a) Bruneau, C. *Angew. Chem., Int. Ed.* **2005**, *44*, 2328–2334. (b) Nieto-Oberhuber, C.; López, S.; Jiménez-Núñez, E.; Echavarran, A. M. *Chem. Eur. J.* **2006**, *12*, 5916–5923.

(11) Steiner, T. *Angew. Chem., Int. Ed.* **2002**, *41*, 48–76.

(12) Bader, R. F. W. *Atoms in Molecules: A Quantum Theory*; Clarendon Press: Oxford, U.K., 1990.

TABLE 1. Free-Energy Differences in Solution (DCE) (in kcal mol⁻¹) of the Structures Involved in the First Step (Path II) Relative to the Reactant Complex (Structure A)^a

substrate	structure		
(2 <i>S</i>)-1	A	0.00	0.00
	TS	3.51	5.43
	E	-20.24	-18.84
(2 <i>R</i>)-1	A	0.00	0.00
	TS	4.48	4.97
	E	-25.68	-24.75
(2 <i>S</i>)-3	A	0.00	0.00
	TS	6.28	7.19
	E	-22.88	-22.35
(2 <i>S</i>)-6	A	0.00	0.00
	TS	6.02	6.77
	E	-21.64	-20.26

^a Series “a” and “b” refer to cyclopropanation on each of the two alkene faces.

the bond critical point $\rho_{\text{bcp}} = 0.0124$ au).¹³ It is known that there is a linear relationship between the electron density at the bond critical point and the stability of the H-bond. On the basis of the study by Parthasarathi et al.¹⁴ on the correlation between the electron density and the Laplacian of the electron density values at the hydrogen bcp and the strength of H-bond, we have estimated the interaction energy from the computed ρ_{bcp} value as 1.96 kcal mol⁻¹, which further supports the effect of this interaction on the selectivity.

The fact that this stabilizing interaction may be significant for the stereoselectivity is confirmed by the transition structures computed for **3** showing *S* configuration at the propargylic center. As expected, a similar interaction is found for the analogous transition structure (2*S*)-3TS_a (C–H···O distance of 2.483 Å). It leads to a kinetic preference for the formation of the cyclopropyl-intermediate (2*S*)-3E_a, although the computed barriers over both faces differ by only 0.9 kcal mol⁻¹, less than for (2*S*)-1. In view of these results, this decreased stereoselectivity may be due to the absence of the isopropyl group and hence of the destabilizing steric interaction induced by this group.

According to these observations, a precursor lacking such C_{sp2}–H···O interaction, as **6**, should undergo an unselective process. However, a synergistic effect of the *gem*-dimethyl substituents and the allylic methyl group induces an eclipsed

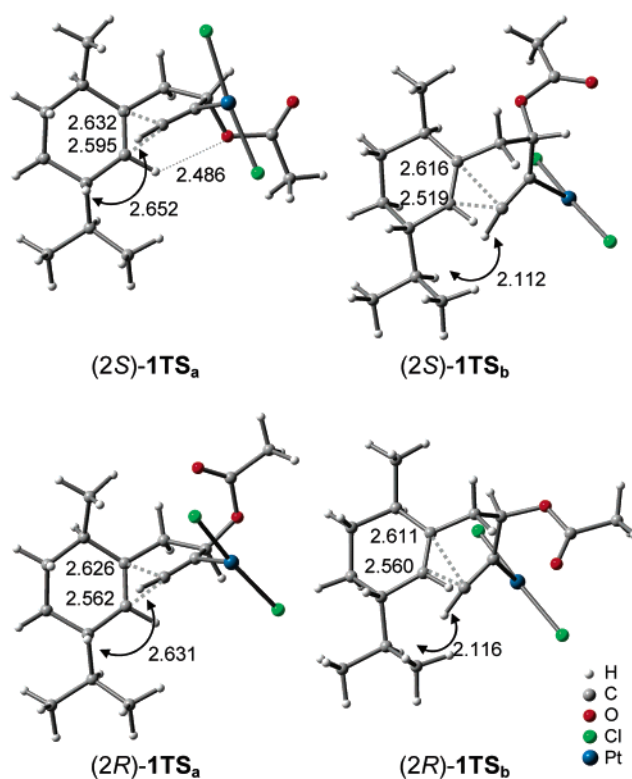


FIGURE 1. Optimized transition structures of the cyclopropanation step for precursor **1** (distance values shown in Å). Suffixes “a” or “b” refer to cyclopropanation on each of the two alkene faces.

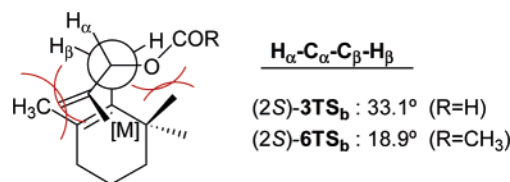


FIGURE 2. Newman projection of the transition structure for (2*S*)-epimers viewed from the direction along the C_α–C_β bond.

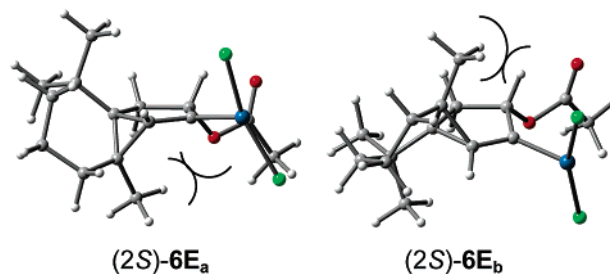


FIGURE 3. Optimized structures of the metallo-carbenoid intermediates for the Pt(II)-mediated cycloisomerization of substrate **6**.

arrangement along the C_α–C_β tether chain for (2*S*)-6TS_b (Figure 2), which could account for its destabilization and for the kinetically favored cyclopropanation through (2*S*)-6TS_a (Table 1).

The results outlined above suggest that subtle intramolecular interactions in the cyclopropanation transition state may be responsible for a substrate-dependent stereoselectivity.

Fehr and Galindo⁷ found that the PtCl₂-catalyzed cycloisomerization of **6** gave the expected rearranged ester **7** plus a

(13) Computed at the MP2/aug-cc-pVDZ/LANL2DZ level.

(14) Parthasarathi, R.; Subramanian, V.; Sathyamurthy, N. *J. Phys. Chem. A* **2006**, *110*, 3349–3351. We thank a referee for calling our attention to this paper.

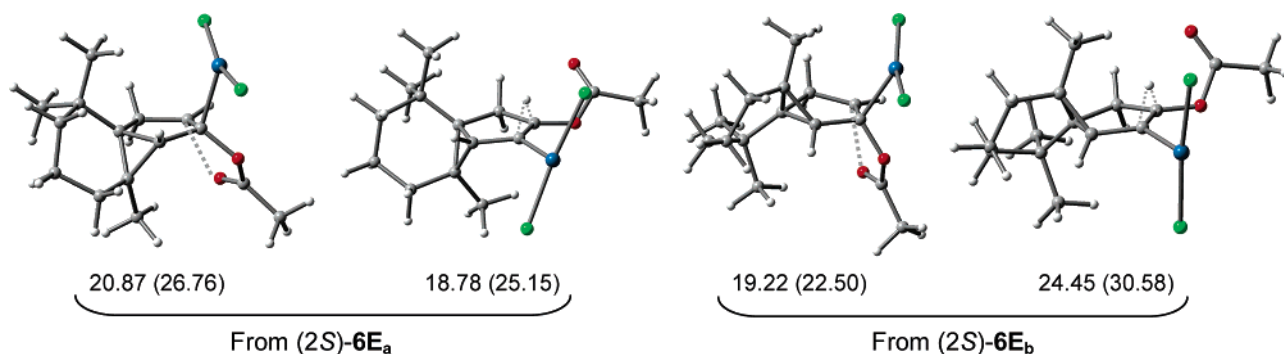


FIGURE 4. Optimized transition structures for the [1,2]-migration from intermediates (2*S*)-**6E**. Activation barriers relative to **6E** are shown (in kcal mol⁻¹) in solution and in gas phase (in parenthesis).

novel, non-rearranged product **8** showing chirality transfer (Scheme 2). Both kinds of cycloisomerizations could be closely related from a mechanistic point of view.^{15a} Thus, for propargylic heterofunctionalized precursors, the endo-cyclization (**E**, Scheme 1) may be followed by a [1,2]-migration of the propargylic moiety to the internal acetylenic position to afford bicyclo[n.1.0] carboxylic ester derivatives.¹⁵ Propargylic esters have been known to yield ester-rearranged products, and so a [1,2]-acyl migration (**D**, Scheme 1) from the key intermediate is favored over a [1,2]-H shift (**I**, Scheme 1). These findings support the experimental results^{6,7} and our previous computed barriers for both migrations for uncrowded acyclic precursors (12.58 vs 17.28, respectively, in gas phase).^{15a} Hence, the unusual formation of **8** from the propargylic ester **6** merits further consideration. A closer inspection of the diastereomeric cyclopropyl metal-carbenoids **6E_a** and **6E_b** (Figure 3) suggests a more sterically impeded [1,2]-acyl migration for (2*S*)-**6E_a** because of the methyl substituent. Under these circumstances, a [1,2]-H shift becomes a competitive pathway. In contrast, the isomer (2*S*)-**6E_b**, displays a lower steric hindrance to the acyl migration, and the alternative process should be disfavored.

To verify this hypothesis, we have computed the activation barriers for both [1,2]-migrations from the key intermediates (2*S*)-**6E_a** and (2*S*)-**6E_b** (Figure 4). As predicted, the results reveal a preferential [1,2]-hydrogen shift from diastereoisomer (2*S*)-**6E_a**, whereas the alternative acyl migration is obstructed. Conversely, the steric hindrance imposed by the methyl substituent in (2*S*)-**6E_b**, and the lower migrating ability inhibit the H shift, clearly promoting the acyl transfer event (Figure 4). Hence, we may speculate that formation of the non-rearranged product **8**, the kinetically favored structure, takes place mainly from the diastereofacial selective cyclopropanation to (2*S*)-**6E_a**, thus ensuring the transfer of the chiral information to the product, in agreement with experimental evidence. The rearranged product could be formed via (2*S*)-**6E_b**, and in a lesser extent, from (2*S*)-**6E_a**. The fact that the Au(I)-promoted reaction yields the rearranged structure as major product (and similar ee values)⁷ could be attributed to the catalyst arrangement, since the Au(I)-linear complex might allow an easier acyl migration from both faces, as compared with the T-shaped Pt-complex, making the H shift a less competitive event.

To sum up, the results described above support path II as operative mechanism over alternative paths and provide a

rationalization for the stereochemical outcome of the Rautenstrauch cyclopropanation. Our calculations correctly predict that the degree of chirality transfer from the stereogenic center depends on the precursor structure. Thus, subtle intramolecular steric interactions in the cyclopropanation step are responsible for the diastereoselectivity of the cyclopropanation. Therefore, the simple inspection of the structures involved in this step provides useful insights into the evolution of the reaction and estimation of regio- and stereoselectivity. This model should allow a refined understanding of further stereoselective processes mediated by late-transition-metal complexes as well as the rational design of new cyclopropanation catalysts and reactions.

Computational Methods

Calculations have been carried out using Gaussian03 program.¹⁶ To save computational recourses, pivaloate has been replaced by acetate group. Structures have been optimized at DFT level by means of the B3LYP functional.¹⁷ The 6-31G(d) basis set has been applied for all the atoms except Pt, which has been described by LANL2DZ basis set,¹⁸ where the innermost electrons are replaced by a relativistic ECP and the valence electrons are explicitly treated by a double- ζ basis set. The optimized geometries were characterized by harmonic analysis, and the nature of the stationary points was determined according to the number of negative eigenvalues of the Hessian matrix. The intrinsic reaction coordinate (IRC) pathways from the transition structures have been followed using a second-order integration method to verify the connections with the correct local minima.¹⁹ Zero-point vibration energy and thermal corrections (at 298 K, 1 atm) to the energy have been estimated on the basis of the frequency calculations. The solvation energies were calculated on the gas-phase optimized structures with the Conductor Polarizable Continuum Model CPCM²⁰ as implemented in Gaussian03.

Supporting Information Available: Additional results on paths I and III, complete ref 16, energies in gas phase and in solution, and atomic coordinates for the computed structures. This material is available free of charge via the Internet at <http://pubs.acs.org>.

JO062594F

(15) (a) Soriano, E.; Marco-Contelles, J. *J. Org. Chem.* **2005**, *70*, 9345–9353. (b) Soriano, E.; Ballesteros, P.; Marco-Contelles, J. *J. Org. Chem.* **2004**, *69*, 8018–8023.

(16) Frisch, M. J. et al. *Gaussian03*, Revision B.03; Gaussian, Inc.: Pittsburgh PA, 2003. See Supporting Information.

(17) (a) Lee, C.; Yang, W.; Parr, R. *Phys. Rev. B* **1988**, *37*, 785–789. (b) Becke, A. *J. Chem. Phys.* **1993**, *98*, 5648–5652.

(18) Hay, P. J.; Wadt, W. R. *J. Chem. Phys.* **1985**, *82*, 270–283.

(19) (a) Fukui, K. *Acc. Chem. Res.* **1981**, *14*, 363–368. (b) González, C.; Schlegel, H. B. *J. Phys. Chem.* **1990**, *94*, 5523–5527.

(20) Barone, V.; Cossi, M. *J. Phys. Chem. A* **1998**, *102*, 1995–2001.